A comparative evaluation of hydrogenation of 3-butyn-2-ol over Pd/Al$_2$O$_3$ in an oscillatory baffled reactor and a commercial stirred tank reactor

Francisca Navarro-Fuentes, Mark Keane and Xiong-Wei Ni[*]

EPSRC Centre for Continuous Manufacturing and Crystallization (CMAC), Centre for Oscillatory Baffled Applications (COBRA), School of Engineering and Physical Sciences, Heriot-Watt University, Edinburgh, EH14 4AS, U.K.

ABSTRACT

A multiphase catalytic hydrogenation of 3-butyn-2-ol over Pd/Al$_2$O$_3$ to produce 3-buten-2-ol was for the first time investigated in both an oscillatory baffled reactor (OBR) and a commercial stirred tank PARR reactor (STR). Catalytic control was first identified in the STR by evaluating the effects of mixing, initial molar ratio of 3-butyn-2-ol/Pd and temperature on reaction rate. These conditions were then used as the benchmark for a comparable evaluation of the OBR in terms of reactor efficiency (power consumption) and hydrogen utilization (H$_2$ efficiency). Our systematic investigations demonstrate that, due to the enhanced mass transfer in the OBR, it consumes 5 times

1

less power to achieve the same reaction rate; delivers 2.3 times higher H_2 efficiency and 50% less reaction time in comparison to the STR.

KEYWORDS

Heterogeneous catalysis, multiphase hydrogenation, oscillatory baffled reactor, commercial PARR reactor

INTRODUCTION

Hydrogenation is a widely used unit operation in chemical and pharmaceutical industries, [1, 2] constituting 10-20% of the synthesis steps in the manufacturing of fine chemicals. [3] A number of pharmaceutical and agrochemical processes are based on selective hydrogenation of functionalized alkynes to alkenes. [4-8] The production of vitamins [9, 10] involves hydrogenation of alkynols to alkenols where a range of catalytic metals (e.g. Rh, Ni, Pd and Pt) have been tested, [11] with Pd-based catalyst being the most popular one [12-16] due to its selectivity (>97%) [17] and activity even at low hydrogen pressures. [18-20]

Conventional heterogeneous catalytic hydrogenation involves three phases, where reactants (gas and liquid) are catalyzed by a porous solid catalyst. A combination of reaction and transport processes occur concurrently where reactants diffuse through phase boundary layers into catalyst pores; reaction takes place once reagents are adsorbed on the active surface; and products desorb and diffuse back to the bulk phase. [21, 22] Such three-phase hydrogenation processes can severely be restricted by limitations in mass transfer between gas and liquid as well as gas and solid, affecting reaction rate, selectivity and productivity. [23] Stirred tanks, packed/trickle beds and bubble columns are the traditional reactors for hydrogenation where catalysts are either stationary (packed

and trickle beds or coated reactors [24-26]) or mobile (stirred tank reactors). The reaction rate can be influenced by many parameters, such as, the type of catalyst, solvent, mixing, reaction temperature and pressure. When the rest of the conditions is fixed mixing in reactors is thus critical in promoting mass transfer of gas into liquid then to the surfaces of catalysts where uniform hydrogen bubble size distribution with small mean sizes together with prolonged residence times of these bubbles are desirable in minimizing interfacial mass transfer resistances. As a result, hydrogen utilization (or efficiency), defined as the ratio of products formed over H_2 fed, is a direct measure of the efficiency of the mass transfer process, in turn the reaction rate and productivity.

In this work, we focus on an alternative reactor system, namely, oscillatory baffled reactor (OBR) [27-37] due to its increased volumetric mass transfer coefficient (k_La) relative to bubble column [38] and stirred tank reactor [39, 40] and the capability of evenly suspending solid particle. [41-43] We carried out a systematic investigation to evaluate and compare an OBR with a commercial STR PARR reactor (STR); the model multiphase catalytic hydrogenation chosen is the reduction of 3-butyn-2-ol over Pd/Al_2O_3 catalyst to generate 3-buten-2-ol (an intermediate) as the target product; both reactor efficiency and hydrogen utilization are used as the indicators of energy and mass transfer efficiency for different reactor designs. The reaction scheme is shown in **Scheme 1** where sequential hydrogenation can lead to the generation of undesired products: 2-butanol via over-hydrogenation and 2-butanone via double bond migration. Although there have been some confidential industrial trials using OBR for hydrogenation, this paper is the first of its kind in public domain and contains a full systematic evaluation and comparison.

3-butyn-2-ol   3-buten-2-ol   2-butanol
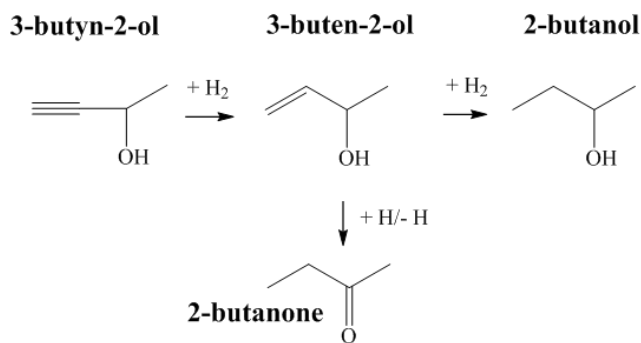
Scheme 1. Reaction scheme for the hydrogenation of 3-butyn-2-ol

EXPERIMENTAL AND ANALYTICAL METHODS

1. Materials

3-butyn-2-ol (97%) was purchased from the Sigma-Aldrich and used as received. Pd/Al$_2$O$_3$ catalyst (1% w/w Pd) was also sourced from Sigma-Aldrich and sieved (ATM fine test sieves) into particle diameter < 45 μm, full characterization can be found elsewhere. [44] Distilled water was the solvent used in this investigation.

2. Reactor configurations

2.1. Commercial PARR STR

The commercial PARR 5500 Series (**Figure 1**) STR comprised of a 100 mL vessel (0.117 m tall, 0.033 m internal diameter and 60 ml working volume) manufactured in T316 stainless steel, fitted with magnetic T316SS stirrer drive unit. The vessel head was equipped with a gauge adapter (pressure gauge 0-14 bar), a vent needle valve, a check valve 14 bar with viton O-ring, a safety rupture disc (Inconel, 1000psi), a gas inlet needle valve, a liquid sampling needle valve and a stirrer drive shaft with straight four-bladed impeller. The H$_2$ was supplied via a gas sparge tube and

quantified by a gas flowmeter (Bronkhorst), no gas induction system was utilized. An internal dip tube with 5 microns sintered Mott filter was used for sampling, which along with a thermocouple (J-type) acted effectively as baffles. A variable speed motor provides the studied stirring speeds (700-1600 rpm). An aluminum block heater was employed, and the temperature was controlled by the Series 4848 Controller.
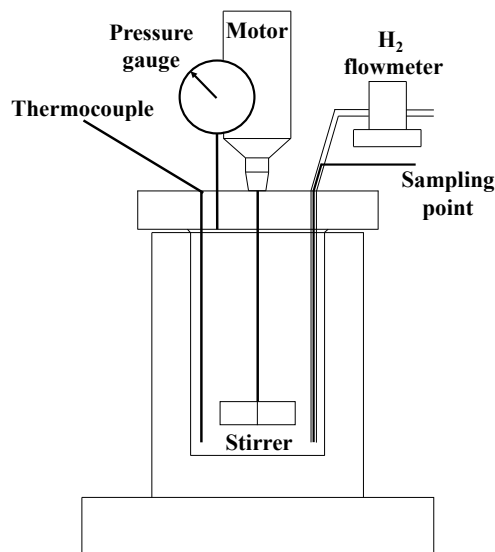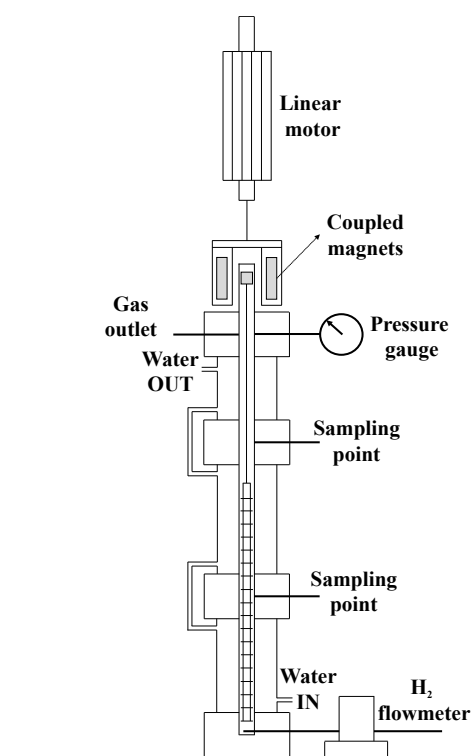

Figure 1. Schematic diagram of the PARR STR

2.2. Oscillatory Baffled Reactor

The OBR in **Figure 2** consisted of a jacketed stainless-steel column of 0.016 m internal diameter and 1.70 m tall. The baffles were spaced 0.025 m apart with a thickness of 0.002 m and a free cross-sectional area ratio of 25%. Oscillation was provided by a linear motor (NiTech Solutions) placed at the top of the column connected to an outer magnetic ring. It was equipped with a set of 42 PFTE baffles supported by two PTFE rods, which are attached to an internal magnet placed at the top of the column. The coupled movement of the two magnets delivered oscillatory mixing under pressures. The oscillatory frequency and amplitude, ranging from 1-5 Hz and up to 12.5 mm

(peak-to-centre) respectively, can be achieved by a programmed control box. The working volume in the reactor was 200 ml. Temperature was kept constant by three jacketed sections that are connected to water bath and recirculator (Grant). The H_2 was supplied via a tubular-shape sparger at the base of the column and quantified by a gas flowmeter (Bronkhorst), no gas induction system was utilized. The pressure within was measured by pressure gauge 0-14 bar. The reactor was secured to a metal structure to minimize mechanical vibrations (not shown in the schematic diagram).

Figure 2. Schematic diagram of the OBR

3. Experimental procedure and analytical method

At the beginning of each experiment, a 0.19 M solution of 3-butyn-2-ol/distilled water with catalyst was charged into the reactor. The volume ratio of gas/liquid was kept the same for both

reactors. The slurry was agitated in an inert atmosphere filled with N_2, and the temperature stabilized. Hydrogen pressure was firstly set by means of a gas regulator and the inlet valve was opened so hydrogen was then introduced (time t=0 for reaction). During the reaction, liquid samples (0.3 mL each) were withdrawn with a maximum total sample volume <10% of the total reaction volume, ensuring that sampling volume is minimized to avoid interference with reaction kinetics. Before gas chromatographic analysis, a standard solution (0.15 M 1-pentanol/distilled water) was added (as internal standard) to samples. The catalyst was not reused in this study.

The analysis of the samples was carried out in a Perkin-Elmer Auto System XL gas chromatograph with an auto sampler equipped with a flame ionization detector (FID) and a Stabilwax® column with the following characteristics: internal diameter = 0.32 mm, length = 30 m, film thickness = 0.25 μm. The carrier gas (He) was pressurized at 10 psig, the temperature in the injector and FID were 533 K and 548 K respectively and the temperature in the oven was held at 313 K for 1 min and then increased to 383 K at a rate of 8 K min^{-1}. The peak areas were converted to mols using regression equations based on calibration, with a detection limit that corresponds to a feedstock concentration <1% molar. A total mass balance was used to determine the concentration of organic species (3-butyn-2-ol, 3-buten-2-ol, 2-butanol and 2-butanone) in the reaction mixture. An overall analytic reproducibility was better than ±5% in the carbon mass balance for repeated reactions. The conversion (**Eq. 1**) and product selectivity (**Eq. 2***)* are calculated via:

$$X\left(\%\right)=\frac{c_{A_0}-c_A}{c_{A_0}}\cdot 100 \qquad\qquad \textbf{(Eq. 1)}$$

$$S\left(\%\right)=\frac{c_i}{c_{A_0}-c_A}\cdot 100 \qquad\qquad \textbf{(Eq. 2)}$$

Where C_{A0}, C_A and C_i are the initial reactant concentration, the reactant and product i concentration at a specific reaction time, respectively. The target product (3-buten-2-ol) selectivity was independent of the working conditions or reactor design and remained above 97% for all the runs, indicating that the hydrogenation reaction was no limited by internal mass transfer. [24]

The initial reaction rate (**Eq. 3**) was defined as the consumption of reactant per unit time and per mass of palladium up to a conversion of 20%, as:

$$r_o = \frac{\dfrac{\Delta n_A}{\Delta t}}{m_{Pd}}$$ (**Eq. 3**)

Power consumption (or power dissipation rate) for both OBR (**Eq. 4**) and STR (**Eq. 5**) was evaluated using the following equations: [39]

$$\frac{P}{V} = \frac{2}{3} \frac{N_b \rho}{\pi C_D^2} \frac{1-\alpha^2}{\alpha^2} x_o^3 \omega^3$$ (**Eq. 4**)

$$\frac{P}{V} = \frac{P_o \rho N^3 D_S^5}{\pi D_v^2 L_h / 4}$$ (**Eq. 5**)

Where P/V is the power dissipation rate per volume (W m^{-3}), N_b the number of baffles per unit length in OBR (m^{-1}), α the ratio of the effective orifice area to the tube area, ρ the density of the fluid (kg m^{-3}), x_o the oscillation amplitude (m), ω the angular oscillation frequency (radians s^{-1}), C_D the orifice discharge coefficient (taken as 0.7), P_o the power number for the impeller depending on the impeller type and dimensions (= 3.5 in this work); N the rotational speed of the stirrer in STR (s^{-1}) and L_h the height of the liquid in STR (m), D_s and D_v are the diameters of the agitator and vessel (m), respectively. The commercial PARR STR was equipped with two baffles (n_B)

whose width (B_w) related to D_v is 0.14. Consequently, the power consumption without baffles $(P/V)_o$ described in **Eq. 5** has to be adjusted to take into account the increase in power consumption caused by the baffles $(P/V)_B$. [45] In this case, $(P/V)_B/(P/V)_o = 12.5$.

RESULTS AND DISCUSSION

1. **Benchmark in PARR STR**

Multiphase catalytic hydrogenations are generally limited by mass transfer, given that hydrogen has to diffuse from the gas phase to the surface of solid catalysts surrounded by liquid through the G/L and L/S interphases. Therefore, it is highly important to study parameters affecting the catalytic performance and identify the conditions where mass transfer is impeded.

1.1. Effect of Mixing

Mass transfer is influenced by mixing that breaks up bubbles, increases surface area [46] and suspends catalyst particles. At a sufficiently high rate of agitation, mass transport effects are minimized. [47] The influence of stirring speed on the initial reaction rate is evaluated by plotting the initial rate vs the power density as shown in **Figure 3**. An increase in r_o is observed with the increase of power density up to 29500W m^{-3}, beyond which r_o is unaffected, indicating that the reaction is under catalytic control.
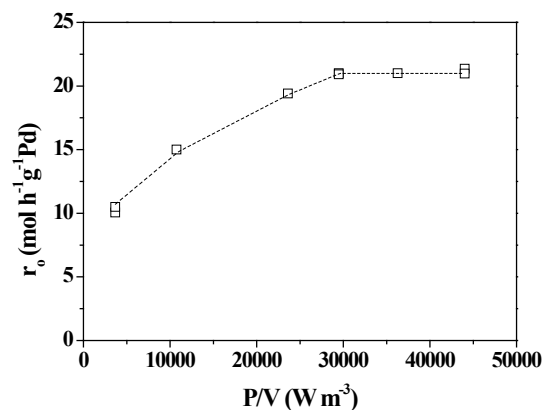
Figure 3. Effect of power density (P/V) on initial reactor rate (r_o). Reaction conditions: initial molar ratio 3-butyn-2-ol/Pd = 6100, temperature = 305 K

1.2. Effect of catalyst amount

The rate is directly proportional to the catalyst loading for reactions that are catalytically controlled. [48] The effect of catalyst amount on the reaction rate is evaluated by plotting the reciprocal of the initial reaction rate (r_o^{-1}) against the initial molar ratio of 3-butyn-2-ol/Pd in **Figure 4**. The results suggest that, at low catalyst amounts (high initial molar ratio of 3-butyn-2-ol/Pd), the reciprocal rate is a linear function of the initial molar ratio of 3-butyn-2-ol/Pd; the diffusion resistance is nearly negligible, and the reaction approaches catalytic control. For the initial molar ratio of 3-butyn-2-ol/Pd less than 1360 (high catalyst loading), the reciprocal rate is independent of the molar ratio, denoting mass transfer controlling the hydrogenation reaction. This is consistent with previous work. [23] [48]
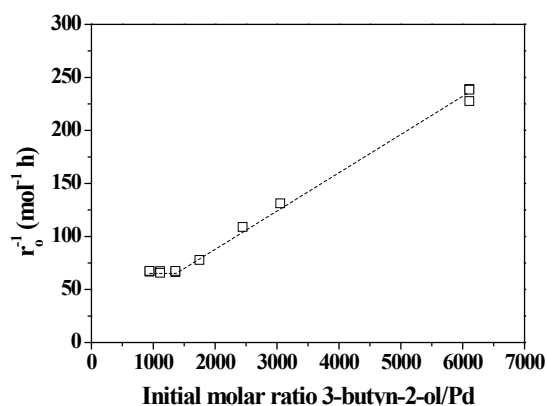
Figure 4. Effect of catalyst amount on the initial reaction rate (r_o). The reciprocal of the initial reaction rate (r_o^{-1}) is plotted as a function of the initial molar ratio 3-butyn-2-ol/Pd. Reaction conditions: $P/V = 29500$ W m^{-3} and temperature = 305 K

1.3. Effect of temperature

The rate of catalytic reactions is strongly dependent on temperature, while mass transfer coefficient is a weak function of temperature. Consequently, the influence of temperature on reaction rate is notable when reactions are under conditions of catalytic control. [48] **Figure 5** plots the initial reaction rate as a function of reaction temperature using reaction conditions that have led to catalytic control from the above. We see that r_o increases with increasing reaction temperature, indicating that the reaction is under catalytic control. However, the influence of external mass transfer becomes noticeable when temperature is above 323K where the concentration of hydrogen in catalyst surface decreases, resulting in no further improvement in reaction rate. For our comparative investigation, 323 K was selected as the basis when the reaction rate is maximized.
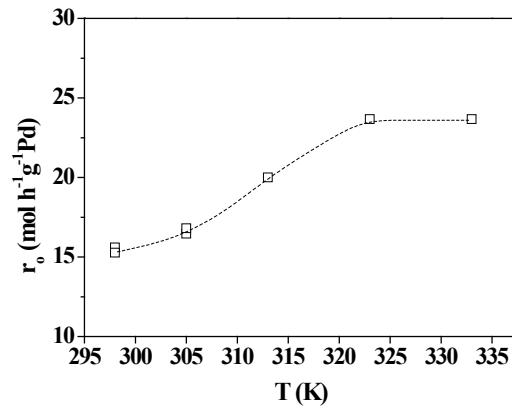
Figure 5. Effect of temperature (T) on the initial reaction rate (r_o). Reaction conditions: initial molar ratio 3-butyn-2-ol/Pd = 1360 and P/V = 29500 W m^{-3}

In summary, the benchmarking conditions leading to catalytic control in the STR are:

- Power density of P/V = 29500 W m^{-3}

- Initial molar ratio of 3-butyn-2-ol/Pd = 1360

- Reaction temperature = 323 K

2. OBR

2.1. Effect of mixing and pressure

The effects of oscillatory mixing on the initial reaction rate (r_o) are plotted in **Figure 6** as a function of frequency for different amplitudes and pressures. When the reactor system is under oscillation, the movement of the baffles creates a periodic acceleration and deceleration of the flow, [49] leading to chaotic mixing where the length of vortices is controlled by the amplitude and

the periodicity of eddy motions by the frequency.[50] The r_o increases with an increase in the frequency. At low frequencies, the increase is negligible but it becomes pronounced at higher frequencies, even more for higher amplitudes[51] and pressures. The intensive and uniform mixing increases the breakup of bubbles, leading to reduction in bubble size, and increase in bubble residence time and gas holdup since the bubbles are trapped in the vortices for longer times, as a result, mass transfer rate and in turn the r_o are enhanced due to the combined effect of frequency and amplitude.[52]
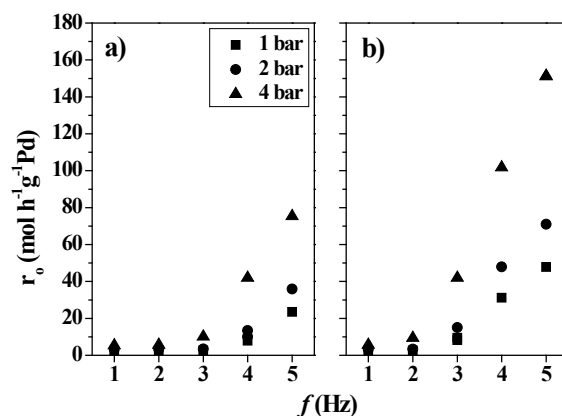
Figure 6. Effect of oscillatory frequency (f) on the initial reaction rate (r_o) at different pressures. Working conditions: initial molar ratio 3-butyn-2-ol = 1360, temperature = 323 K and oscillatory amplitude: a) x_o = 9 mm and b) x_o = 12.5 mm
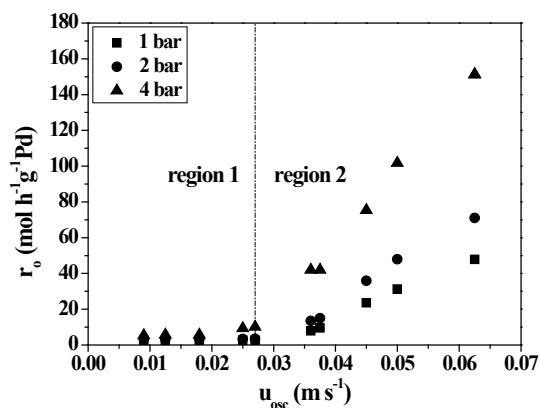
Figure 7. Effect of oscillatory velocity (u_{osc}) on initial reaction rate (r_o) at different pressures. Working conditions: initial molar ratio 3-butyn-2-ol/Pd = 1360 and temperature = 323 K

The combined effect in terms of oscillatory velocity ($x_o f$) on the reaction rate is shown in **Figure 7**. It suggests that two regions exist: in region 1 corresponding to low oscillatory velocities, r_o is independent of mixing as bubble holdup and breakup are not promoted, regardless the working pressure. At higher oscillatory velocities in region 2, r_o is significantly enhanced due to improvements in bubble mean size and size distributions, bubble residence time and gas holdup, more pronounced at higher pressures. This pattern has been reported previously. [53] Concentration profiles of the two regions can be found in Supporting Information (**Figure S1**).

3. Comparison of PARR STR and OBR

3.1. Reactor efficiency profile

The reactor efficiency is evaluated by plotting the initial reaction rate as a function of energy dissipation per unit mass of the system (W/m^{-3}). **Figure 8** shows the comparison for both reactors under the same initial molar ratio of 3-butyn-2-ol/Pd = 1360 and the same reaction temperature,

but at different pressures. We see the rising profiles of the initial reaction rate against power density (mixing) for all conditions tested, indicating that the hydrogenation of 3-butyn-2-ol in the OBR is still dominated by mass transfer under these oscillation conditions. Note that it was not possible to operate at higher oscillation amplitudes and frequencies that allow the catalytic control to be achieved for the setup of the OBR, as the maximum oscillation frequency and amplitude were employed. Even under mass transfer limitations, about 6 times less power dissipation in the OBR is required to achieve the same reaction rate obtained in the STR working at the same pressure (arrows with dashed lines) and about 3 times less power dissipation if the operating pressure in the OBR is halved (arrows with dotted lines), hence representing a promising energy-efficient platform for G/L reactions as previously reported. [40, 54]
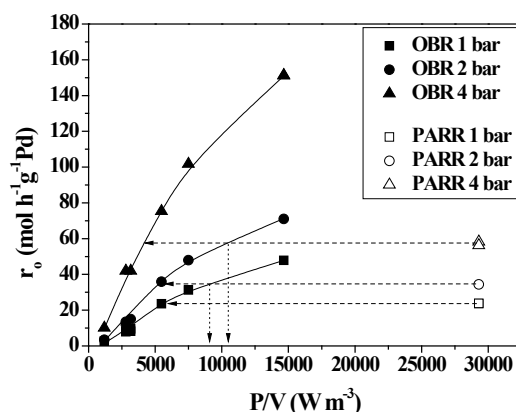
Figure 8. Effect of power density (P/V) on initial reaction rate (r_o) at different pressure in PARR STR and OBR. Working conditions: initial molar ratio 3-butyn-2-ol/Pd = 1360 and temperature = 323 K

3.2. H_2 utilization

The key focus of this work is to compare H_2 utilization for the two reactors as it is directly linked to the efficiency of multiphase mass transfer (dominated by gas-liquid phase resistence). The H_2 efficiency (%) is defined as mol of products formed to mol of hydrogen fed into the reactor for a fixed reaction time. **Table 1** compiles the H_2 efficiency and reaction time at which 95% conversion is achieved for both reactors. Note that the comparison is performed under the same initial molar ratio of 3-butyn-2-ol/Pd (= 1360), the same reaction temperature (323 K) and the same catalyst loading in both reactors (the initial molar ratio 3-butyn-2-ol/Pd in the OBR = 4525), but the power consumption in the OBR is about half of the benchmark conditions in the PARR.

Table 1. H_2 efficiency and reaction time (RT) for PARR and OBR. Working conditions: **(P/V)**_{PARR} = **29300 W m⁻³**, **(P/V)**_{OBR[max]} = **14650 W m⁻³**, temperature = 323 K, RT at X = 95%

PARR STR				
Run no.	*Pressure, bar*	*Initial molar ratio 3-butyn-2-ol/Pd*	*RT, min*	*H_2 efficiency, %*
1	1	1360	23	29
2	2	1360	16	31
3	4	1360	9.4	34
OBR				
Run no.	*Pressure, bar*	*Initial molar ratio 3-butyn-2-ol/Pd*	*RT, min*	*H_2 efficiency, %*
4	1	1360	12.5	67
5	2	1360	8	71
6	4	1360	4	77

7	1	4525	16.5	49
8	2	4525	11	53
9	4	4525	6	59

Effect of pressure. The effect of pressure is evaluated by comparing the performance of each reactor at different pressures. In the PARR STR, a H_2 efficiency of 29% is obtained at atmospheric pressure (see run no. 1), which is increased by 7% when pressure is doubled from 1 to 2 bar and by 10% from 2 to 4 bar with the correspondent reaction time reduction of 30% and 40 %, respectively (see runs no. 2, 3).

At the same working conditions, the H_2 efficiency in the OBR is 67% at ambient pressure (see run no. 4), which is increased by 7% when pressure is doubled from 1 to 2 bar and by 10% from 2 to 4 bar with the correspondent reaction time reduction of 40% and 50 %, respectively (see runs no. 5, 6).

The percentage increase in the H_2 efficiency is unchanged for the increase of pressures when the same catalyst loading was used in the OBR (see runs no. 7-9). This indicates that the effect of pressure is purely on the enhancement of the solubility of H_2 in water in the multiphase catalytic hydrogenation; when pressure is doubled, the H_2 efficiency increases 3% regardless of reactor configurations.

Effect of mixing. The effect of mixing is evaluated by comparing the performance of both reactors under the same pressure. For the same initial molar ratio of 3-butyn-2-ol/Pd, the H_2 efficiency in the OBR was increased by 2.3 times and reaction time reduced by half in comparison to that in the PARR STR (see runs 1-3 vs 4-6), irrespective of operational pressures. These

improvements are entirely due to the enhancement of mixing. Likewise, for the same catalyst loading in the two reactors (effectively 70% lesser catalyst in the OBR), the OBR delivered a 70% improvement in the H_2 efficiency and a 30% reduction in the reaction time with respect to the PARR STR (see runs 1-3 vs 7-9). This is in agreement with the reported enhanced k_La in OBR.

CONCLUSIONS

We report a systematic comparison of hydrogen utilization and reactor efficiency in the model catalytic hydrogenation of 3-butyn-2-ol to 3-buten-2-ol over Pd/Al_2O_3. Benchmarking conditions in the commercial PARR STR are firstly established for a range of operational parameters where the reaction is under catalytic control. By applying these conditions to the OBR, rising profiles of the initial reaction rates against power density (mixing intensity) are observed, this indicates that the hydrogenation reaction in the OBR is still under mass transfer control. At the same operating pressure, the OBR requires about 6 times less power consumption to achieve the same reaction rate as STR does. Furthermore, the reaction rate obtained in the STR can be attained in the OBR at half the operating pressures with 3 times efficient in power dissipation rate, due to enhanced mass transfer.

The operating pressure only affects the solubility of H_2 in water, leading to the same 3% increase in H_2 efficiency and the same 10% reduction in reaction time when the pressure was doubled, independent of the reactor configuration. The enhanced oscillatory mixing in the OBR brings about 2.3 times increase in H_2 efficiency and a 50% reduction in reaction time comparing the benchmark cases. While at the same catalyst loading in both reactors, i.e. 70% lesser catalyst in the OBR, the improvement includes 70% better in H_2 efficiency and 30% shorter in reaction time. All the above

comparisons are based on un-equal power dissipation rates where it is about half in the OBR than that in the STR, indicating that the OBR is an energy efficient reactor platform.

AUTHOR INFORMATION

Corresponding Author:

[*] Tel: 00441314513781, Email: x.ni@hw.ac.uk

SUPPORTING INFORMATION

Figure S1. Variation in the concentration of reactant (C_A) during the hydrogenation (h) in the two regions: **a)** low mixing (u_{osc} = 0.009 m s^{-1}) and **b)** high mixing (u_{osc} = 0.0625 m s^{-1}) at different pressures.

NOMENCLATURE

Roman symbols

C_A: reactant concentration, mol L^{-1}

C_{Ao}: initial reactant concentration, mol L^{-1}

C_D: orifice discharge coefficient, dimensionless

C_i: concentration of species i, mol L^{-1}

D_s: diameter of the stirrer, m

D_v: diameter of PARR vessel, m

f: oscillation frequency, Hz

L_h: height of the liquid in PARR, m

m_{Pd}: mass of palladium, g

N: rotational speed of the stirrer, s^{-1}

n_A: mol of reactant, mol

N_b: number of baffles per unit length in OBR, m^{-1}

n_B: number of baffles in PARR

P: power required for mixing, W

P_o: power number for PARR, dimensionless

(P/V): power consumption or power dissipation rate, W m^{-3}

r_o: initial reaction rate, mol h^{-1} g^{-1}Pd

RT: reaction time at X = 95%, min

S (%): percentage selectivity, dimensionless

t: reaction time, h

V: total liquid volume in the reactor, m^3

W_B: baffles width in PARR, m

X (%): percentage conversion, dimensionless

x_o: oscillation amplitude (peak-to-centre), m

Greek symbols

α: ratio of the effective baffle orifice area to the tube area, dimensionless

ρ: density of the fluid, $kg \; m^{-3}$

ω: angular oscillation frequency, $radians \; s^{-1}$

Abbreviations

OBR: oscillatory baffled reactor

PARR: commercial PARR STR

STR: stirred tank reactor

G: gas

L: liquid

REFERENCES

1. Blaser, H.-U.; Malan, C.; Pugin, B.; Spindler, F.; Steiner, H.; Studer, M., Selective Hydrogenation for Fine Chemicals: Recent Trends and New Developments. Advanced Synthesis & Catalysis 2003, 345, 103-151.

2. Mills, P. L.; Chaudhari, R. V., Multiphase catalytic reactor engineering and design for pharmaceuticals and fine chemicals. Catalysis Today 1997, 37, 367-404.

3. Roessler, F., Catalysis in the industrial production of pharmaceuticals and fine chemicals. CHIMIA International Journal for Chemistry 1996, 50, 106-109.

4. Nijhuis, T.; Van Koten, G.; Moulijn, J., Optimized palladium catalyst systems for the selective liquid-phase hydrogenation of functionalyzed alkynes. Applied Catalysis A: General 2003, 238, 259-271.

5. Spee, M. P.; Boersma, J.; Meijer, M. D.; Slagt, M. Q.; van Koten, G.; Geus, J. W., Selective liquid-phase semihydrogenation of functionalized acetylenes and propargylic alcohols with silica-supported bimetallic palladium-copper catalysts. The Journal of organic chemistry 2001, 66, 1647-1656.

6. Marín-Astorga, N.; Alvez-Manoli, G.; Reyes, P., Stereoselective hydrogenation of phenyl alkyl acetylenes on pillared clays supported palladium catalysts. Journal of Molecular Catalysis A: Chemical 2005, 226, 81-88.

7. Aramendia, M.; Borau, V.; Jimenez, C.; Marinas, J.; Sempere, M.; Urbano, F.; Villar, L., Study of the Selective Semi-Hydrogenation of Various Carbon-Carbon Triple Bonds Over a Pd/Sepiolite Catalyst. In Studies in Surface Science and Catalysis, Elsevier 1993, 75, 2435-2438.

8.   Joannet, E.; Horny, C.; Kiwi-Minsker, L.; Renken, A., Palladium supported on filamentous active carbon as effective catalyst for liquid-phase hydrogenation of 2-butyne-1,4-diol to 2-butene-1,4-diol. Chemical Engineering Science 2002, 57, 3453-3460.

9.   Bonrath, W.; Eggersdorfer, M.; Netscher, T., Catalysis in the industrial preparation of vitamins and nutraceuticals. Catalysis Today 2007, 121, 45-57.

10.   Bonrath, W.; Netscher, T., Catalytic processes in vitamins synthesis and production. Applied Catalysis A: General 2005, 280, 55-73.

11.   Chen, B.; Dingerdissen, U.; Krauter, J. G. E.; Lansink Rotgerink, H. G. J.; Möbus, K.; Ostgard, D. J.; Panster, P.; Riermeier, T. H.; Seebald, S.; Tacke, T.; Trauthwein, H., New developments in hydrogenation catalysis particularly in synthesis of fine and intermediate chemicals. Applied Catalysis A: General 2005, 280, 17-46.

12.   Vernuccio, S.; von Rohr, P. R.; Medlock, J., General Kinetic Modeling of the Selective Hydrogenation of 2-Methyl-3-butyn-2-ol over a Commercial Palladium-Based Catalyst. Industrial & Engineering Chemistry Research 2015, 54, 11543-11551.

13.   Prestianni, A.; Crespo-Quesada, M.; Cortese, R.; Ferrante, F.; Kiwi-Minsker, L.; Duca, D., Structure sensitivity of 2-methyl-3-butyn-2-ol hydrogenation on Pd: computational and experimental modeling. The Journal of Physical Chemistry C 2014, 118, 3119-3128.

14.   Elias, Y.; Rudolf von Rohr, P.; Bonrath, W.; Medlock, J.; Buss, A., A porous structured reactor for hydrogenation reactions. Chemical Engineering and Processing: Process Intensification 2015, 95, 175-185.

15.   Cherkasov, N.; Ibhadon, A. O.; McCue, A. J.; Anderson, J. A.; Johnston, S. K., Palladium–bismuth intermetallic and surface-poisoned catalysts for the semi-hydrogenation of 2-methyl-3-butyn-2-ol. Applied Catalysis A: General 2015, 497, 22-30.

16.   Bruehwiler, A.; Semagina, N.; Grasemann, M.; Renken, A.; Kiwi-Minsker, L.; Saaler, A.; Lehmann, H.; Bonrath, W.; Roessler, F., Three-Phase Catalytic Hydrogenation of a Functionalized Alkyne: Mass Transfer and Kinetic Studies with in Situ Hydrogen Monitoring. Industrial & Engineering Chemistry Research 2008, 47, 6862-6869.

17.   Nikoshvili, L. Z.; Makarova, A. S.; Lyubimova, N. A.; Bykov, A. V.; Sidorov, A. I.; Tyamina, I. Y.; Matveeva, V. G.; Sulman, E. M., Kinetic study of selective hydrogenation of 2-methyl-3-butyn-2-ol over Pd-containing hypercrosslinked polystyrene. Catalysis Today 2015, 256, Part 2, 231-240.

18.   Molnár, Á.; Sárkány, A.; Varga, M., Hydrogenation of carbon–carbon multiple bonds: chemo-, regio- and stereo-selectivity. Journal of Molecular Catalysis A: Chemical 2001, 173, 185-221.

19.   Jones, W. H., Platinum and Palladium in the Pharmaceutical Industry. Platinum Metals Review 1958, 2, 86-89.

20.   Bonrath, W.; Wüstenberg, B.; Schütz, J.; Medlock, J.; Netscher, T., Hydrogenation in the vitamins and fine chemicals industry-an overview. INTECH Open Access Publisher2012.

21.   Beller, M., Catalysis. From Principles to Applications. Wiley Online Library 2013.

22.   Alper, E., Mass transfer with chemical reaction in multiphase systems, volume II: Three-phase systems. AIChE Journal 1983.

23.   Yuan, G.; Keane, M. A., Liquid phase catalytic hydrodechlorination of 2,4-dichlorophenol over carbon supported palladium: an evaluation of transport limitations. Chemical Engineering Science 2003, 58, 257-267.

24.   Cherkasov, N.; Al-Rawashdeh, M. m.; Ibhadon, A. O.; Rebrov, E. V., Scale up study of capillary microreactors in solvent-free semihydrogenation of 2-methyl-3-butyn-2-ol. Catalysis Today 2016, 273, 205-212.

25.   Bai, Y.; Cherkasov, N.; Huband, S.; Walker, D.; Walton, R.; Rebrov, E., Highly Selective Continuous Flow Hydrogenation of Cinnamaldehyde to Cinnamyl Alcohol in a Pt/SiO_2 Coated Tube Reactor. Catalysts 2018, 8, 58.

26.   Lokhat, D.; Domah, A. K.; Padayachee, K.; Baboolal, A.; Ramjugernath, D., Gas–liquid mass transfer in a falling film microreactor: Effect of reactor orientation on liquid-side mass transfer coefficient. Chemical Engineering Science 2016, 155, 38-44.

27.   Eze, V. C.; Phan, A. N.; Pirez, C.; Harvey, A. P.; Lee, A. F.; Wilson, K., Heterogeneous catalysis in an oscillatory baffled flow reactor. Catalysis Science & Technology 2013, 3, 2373-2379.

28.   Wilson, B.; Ni, X.; Sherrington, D. C., On the Investigation of a Phase-Transfer Catalysis Reaction in an Oscillatory Baffled Reactor. Industrial & Engineering Chemistry Research 2001, 40, 5300-5304.

29.   Wilson, B.; Sherrington, D. C.; Ni, X., Butylation of Phenylacetonitrile in an Oscillatory Baffled Reactor. Industrial & Engineering Chemistry Research 2005, 44, 8663-8670.

30.   Ni, X.; Murray, K. R.; Zhang, Y.; Bennett, D.; Howes, T., Polymer product engineering utilising oscillatory baffled reactors. Powder Technology 2002, 124, 281-286.

31.   Rasdi, F. R. M.; Phan, A. N.; Harvey, A. P., Rapid Determination of the Reaction Kinetics of an n-Butylbenzaldimine Synthesis Using a Novel Mesoscale Oscillatory Baffled Reactor. Procedia Engineering 2012, 42, 1527-1539.

32.   Zheng, M.; Skelton, R. L.; Mackley, M. R., Biodiesel Reaction Screening Using Oscillatory Flow Meso Reactors. Process Safety and Environmental Protection 2007, 85, 365-371.

33.   Rasdi, F. R. M.; Phan, A. N.; Harvey, A. P., Rapid determination of reaction order and rate constants of an imine synthesis reaction using a mesoscale oscillatory baffled reactor. Chemical Engineering Journal 2013, 222, 282-291.

34.   Abbott, M. S. R.; Valente Perez, G.; Harvey, A. P.; Theodorou, M. K., Reduced power consumption compared to a traditional stirred tank reactor (STR) for enzymatic saccharification of alpha-cellulose using oscillatory baffled reactor (OBR) technology. Chemical Engineering Research and Design 2014, 92, 1969-1975.

35.   Loponov, K. N.; Deadman, B. J.; Zhu, J.; Rielly, C.; Holdich, R. G.; Hii, K. K.; Hellgardt, K., Controlled multiphase oxidations for continuous manufacturing of fine chemicals. Chemical Engineering Journal 2017, 329, 220-230.

36.   Eze, V. C.; Fisher, J. C.; Phan, A. N.; Harvey, A. P., Intensification of carboxylic acid esterification using a solid catalyst in a mesoscale oscillatory baffled reactor platform. Chemical Engineering Journal 2017, 322, 205-214.

37.   Ikwebe, J.; Harvey, A. P., Kinetics of Cellulose Hydrolysis in an Oscillatory Baffled Reactor. American Journal of Biomass and Bioenergy 2016, 5, 130-145.

38.   Al-Abduly, A.; Christensen, P.; Harvey, A.; Zahng, K., Characterization and optimization of an oscillatory baffled reactor (OBR) for ozone-water mass transfer. Chemical Engineering and Processing: Process Intensification 2014, 84, 82-89.

39.   Ni, X.; Gao, S.; Cumming, R. H.; Pritchard, D. W., A comparative study of mass transfer in yeast for a batch pulsed baffled bioreactor and a stirred tank fermenter. Chemical Engineering Science 1995, 50, 2127-2136.

40.   Hewgill, M. R.; Mackley, M. R.; Pandit, A. B.; Pannu, S. S., Enhancement of gas-liquid mass transfer using oscillatory flow in a baffled tube. Chemical Engineering Science 1993, 48, 799-809.

41.   Mackley, M. R.; Smith, K. B.; Wise, N. P., The mixing and separation of particle suspensions using oscillatory flow in baffled tubes. Trans. IChem.E. 1993, 71(A), 649-656.

42.   Gao, S.; Ni, X.; Cumming, R. H.; Greated, C. A.; Norman, P. I., Experimental investigation of particle flocculation in a batch oscillatory baffled reactor. Separation Science and Technology 1998, 33, 68-72.

43.   Kacker, R.; Regensburg, S. I.; Kramer, H. J. M., Residence time distribution of dispersed liquid and solid phase in a continuous oscillatory flow baffled crystallizer. Chem. Eng. J. 2017, 317, 413-423.

44. Gómez-Quero, S.; Cárdenas-Lizana, F.; Keane, M. A., Liquid phase catalytic hydrodechlorination of 2,4-dichlorophenol over Pd/Al2O3: Batch vs. continuous operation. Chemical Engineering Journal 2011, 166, 1044-1051.

45. Nagata, S., Mixing—principles and applications. A Halsted press book 1975.

46. Chang, M.-Y.; Morsi, B. I., Mass transfer in a three-phase reactor operating at elevated pressures and temperatures. Chemical Engineering Science 1992, 47, 1779-1790.

47. Bond, G. C., Heterogeneous Catalysis. Principles and Applications. Oxford University Press 1987.

48. Roberts, G., Catalysis in Organic Synthesis. Academic Press, New York 1976, 1-47.

49. Ni, X.; Jian, H.; Fitch, A. W., Computational fluid dynamic modelling of flow patterns in an oscillatory baffled column. Chemical Engineering Science 2002, 57, 2849-2862.

50. Abbott, M. S. R.; Harvey, A. P.; Perez, G. V.; Theodorou, M. K., Biological processing in oscillatory baffled reactors: operation, advantages and potential. Interface Focus 2013, 3, 20120036.

51. Ahmed, S. M. R.; Phan, A. N.; Harvey, A. P., Mass transfer enhancement as a function of oscillatory baffled reactor design. Chemical Engineering and Processing - Process Intensification 2018, 130, 229-239.

52. Oliveira, M. S. N.; Ni, X.-W., Effect of hydrodynamics on mass transfer in a gas–liquid oscillatory baffled column. Chemical Engineering Journal 2004, 99, 59-68.

53.   Oliveira, M. S. N.; Ni, X. W., Characterization of a gas-liquid OBC: Bubble size and gas holdup. AIChE Journal 2004, 50, 3019-3033.

54.   Ni, X.; Gao, S., Mass transfer characteristics of a pilot pulsed baffled reactor. Journal of Chemical Technology & Biotechnology 1996, 65, 65-71.